



ELSEVIER

Spectrochimica Acta Part B 56 (2001) 551–564

SPECTROCHIMICA
ACTA
PART B

www.elsevier.nl/locate/sab

Comparison of modeling calculations with experimental results for direct current glow discharge optical emission spectrometry

Annemie Bogaerts^{a,*}, Ludger Wilken^b, Volker Hoffmann^b,
Renaat Gijbels^a, Klaus Wetzig^b

^a*Department of Chemistry, University of Antwerp, Universiteitsplein 1, B-2610 Wilrijk-Antwerp, Belgium*

^b*Institut für Festkörper- und Werkstofforschung Dresden, Postfach 270016, D-01171 Dresden, Germany*

Received 23 February 2001; accepted 2 May 2001

Abstract

A comparison is made between numerical modeling and experimental results for the electrical characteristics, the erosion rates and the optical emission intensities of various argon and copper lines in a direct current glow discharge, to verify the model calculations and to illustrate some features and limitations of the model. In order to reach good agreement with the current–voltage characteristics, the gas temperature, which was treated as an adjustable parameter, was assumed to increase slightly as a function of voltage and pressure. This assumption is in accordance with theoretical predictions and experimental observations in the literature. The erosion rates and optical emission intensities, calculated as a function of voltage and pressure, were also found to be in reasonable agreement with the experimental data. However, it appeared that still better agreement with the measured data could be reached when the gas temperature was assumed to be constant as a function of voltage. This illustrates that the effect of voltage cannot yet be completely correctly predicted for both the electrical current and the erosion rates and optical emission intensities at the same time, and that, therefore, the glow discharge behavior is not yet perfectly described in the model. This is not unexpected in view of the complexity of the model calculations and the uncertainties of some input data. However, in general, the agreement between model results and experimental data is satisfactory, so that it can be concluded that the model gives already a realistic picture of the direct current glow discharge. © 2001 Elsevier Science B.V. All rights reserved.

Keywords: Direct current glow discharge; Modelling calculations; Optical emission spectrometry; Gas temperature; Erosion rates

* Corresponding author. Tel.: +32-3820-2377; fax: +32-3820-2376.

E-mail address: bogaerts@uia.ua.ac.be (A. Bogaerts).

1. Introduction

In previous years, a comprehensive modeling network has been developed to describe the behavior of various plasma species in a direct current (d.c.) glow discharge used for analytical spectrometry (see [1] and references therein). Typical results of the models include the electrical characteristics, the potential and electric field distributions, the densities, fluxes and energies of the various plasma species, information about collision processes in the plasma and about sputtering at the cathode, optical emission intensities, etc. This modeling network was developed to obtain a better insight in the glow discharge behavior, and to predict how the analytical results might be improved. However, in order to be useful as a predicting tool, the models need to be carefully verified by comparison of the calculation results with experimental data. Measurements in a glow discharge plasma are, however, not very straightforward. Indeed, plasma quantities such as the densities and energies of the plasma species, the potential distribution, and the collision rates in the plasma are very difficult to measure in a glow discharge cell with a volume in the order of 1 cm³. However, the electrical characteristics, the erosion rates due to sputtering at the cathode and the optical emission intensities can be measured more easily, because these are macroscopic quantities. In this paper, we present the comparison between our calculated results and measured data for the electrical current as a function of voltage and pressure, as well as for the erosion rates and optical emission intensities of several argon and copper lines, at a range of voltages and pressures.

2. Short description of the modeling network

An overview of the modeling network has been given in Bogaerts and Gijbels [1], and the detailed models have been explained in the references therein. Therefore, only a short description will be given here. The species assumed to be present in the plasma are the argon gas atoms, the argon ions and fast argon atoms, the argon atoms in various excited levels, the sputtered copper atoms

and the corresponding ions, both in the ground state and in excited levels, and the electrons. These species are described with a combination of Monte Carlo, fluid and collisional–radiative models. The argon gas atoms are assumed to be uniformly distributed in the plasma with thermal velocities, so that no model is used to describe their behavior. The electrons are split up in two groups, depending on their energy: the fast electrons (with energy above 11.55 eV, i.e. the threshold for inelastic collisions with argon atoms) are simulated with a Monte Carlo method, whereas the slow electrons are treated with a fluid approach, together with the argon ions. The latter model also includes Poisson's equation, to obtain a self-consistent electric field distribution (i.e. the electric field which determines the motion of the charged plasma species is calculated from the densities of these species). The fast argon ions in the cathode dark space (CDS, i.e. the region adjacent to the cathode, characterized by a strong electric field) are also followed with a Monte Carlo simulation, as well as the fast argon atoms, which are created in the CDS from elastic collisions of the argon ions with argon gas atoms. The level populations of the argon atoms in 64 different excited levels were calculated with a so-called collisional–radiative model, which consists of a set of balance equations (one for each level) with different production and loss terms. The amount of sputtering at the copper cathode is calculated from the flux energy distributions of fast argon ions, argon atoms and copper ions bombarding the cathode, multiplied with an empirical formula for the sputtering yield as a function of the bombarding energies. When the sputtered copper atoms arrive in the plasma, they are characterized by energies in the order of 5–15 eV. They lose this energy almost immediately by collisions with argon gas atoms, until they are thermalized. This thermalization process is simulated with the Monte Carlo method. This results in a so-called thermalization profile, which gives the number of thermalized sputtered copper atoms as a function of distance from the cathode. The latter is used as input in the model used to describe the further behavior of the copper atoms, i.e. transport by diffusion, and collision processes such as ioniza-

tion and excitation, and the behavior of the excited copper atoms and ions. The model developed for this is again a collisional–radiative model, consisting of a set of balance equations for the different levels (eight copper atomic and seven Cu^+ ionic levels were incorporated, as well as the Cu^{2+} ions). Finally, the behavior of the fast Cu^+ ions in the CDS is also simulated with a Monte Carlo method, in analogy to the Monte Carlo model for the fast Ar^+ ions. All the models are coupled to each other due to the interaction processes between the different species, and they are solved iteratively until final convergence is reached, which can take several days on a Unix workstation.

The modeling network is applied here to the Grimm-type glow discharge cell described below, at a range of different voltages and currents. However, the model geometry is simplified to a cylinder with a diameter of 4 mm and a length of 1.5 cm, because it has been demonstrated that the glow discharge plasma is mainly concentrated in the first centimeter from the cathode in the Grimm-type glow discharge cell [2]. The Monte Carlo models are developed in three dimensions, whereas the fluid and collisional–radiative models are two-dimensional. Indeed, the cylindrical symmetry of the cell investigated allowed us to reduce the three dimensions to two dimensions (axial and radial directions).

3. Experimental set-up

The experiments were carried out with the LECO GDS 750D polychromator equipped with an additional monochromator (Digikrom 480 by CVI Laser Corporation). With the polychromator the lines Cu 219.2 nm, Cu 327.3 nm, Ar 415.8 nm, H 121.5 nm, O 130.2 nm, C 156.1 nm and N 174.2 nm were measured. The measurement of the light elements was included to check good vacuum conditions.

The monochromator allows line intensity measurements in the wavelength range between 200 and 800 nm with a resolution of 0.2 nm and has a wavelength dependent ratio between in- and output intensity. Also, the photomultiplier has a

wavelength dependent sensitivity and the measured signal in the used analogue mode depends on the applied voltage (HS). With the help of a calibration lamp, the determination of the wavelength-dependent sensitivity is possible, but at the time of the measurements, such a calibration lamp was not available. However, to get a rough overview of the absolute intensities, we calculated voltage independent intensities. Fig. 1 shows the calibration curves for different lines. The intensities nearly double when the photomultiplier voltage changes by one step. The measured line intensities of the monochromator (Ex) are transformed into photomultiplier voltage independent intensities (Excor) according to the following equation:

$$\text{Excor} = \text{Ex} \times 2^{(15 - \text{HS})}$$

An alternative way would be to use a constant voltage and neutral density filters in front of the monochromator to ensure linearity of response.

Details of the self-built Grimm-type source [3] with water cooling from the backside of the sample are given in [4]. The anode diameter is 4 mm. A mass flow controller steers the argon gas flow (purity of 99.998%). For the theoretical investigations, the argon pressure in the source must be known. Therefore, the dependence of this pressure on the gas flow at the inlet, given in standard cubic centimeters per minute ($\text{sccm} = \text{cm}^3/\text{min}$), was determined (see Table 1). For this purpose we fixed a vacuum adapter to the plane of the sample, which is connected with a membrane vacuum meter (type VM 101 by Hochvakuum, Dresden). The accuracy of this instrument is better than 10%. Measurements at different parts of the source (not in the pumping line) until now have not shown any differences above this uncertainty. It must be mentioned that all connecting parts for these measurements have diameters above 2 mm. Therefore, possible differences, e.g. near the ring slit, cannot be detected and the given pressures represent average values.

The internal voltage supply of the instrument was used with an accuracy of the recorded voltages and currents better than 5%.

To get similar plasma conditions, all sputtered

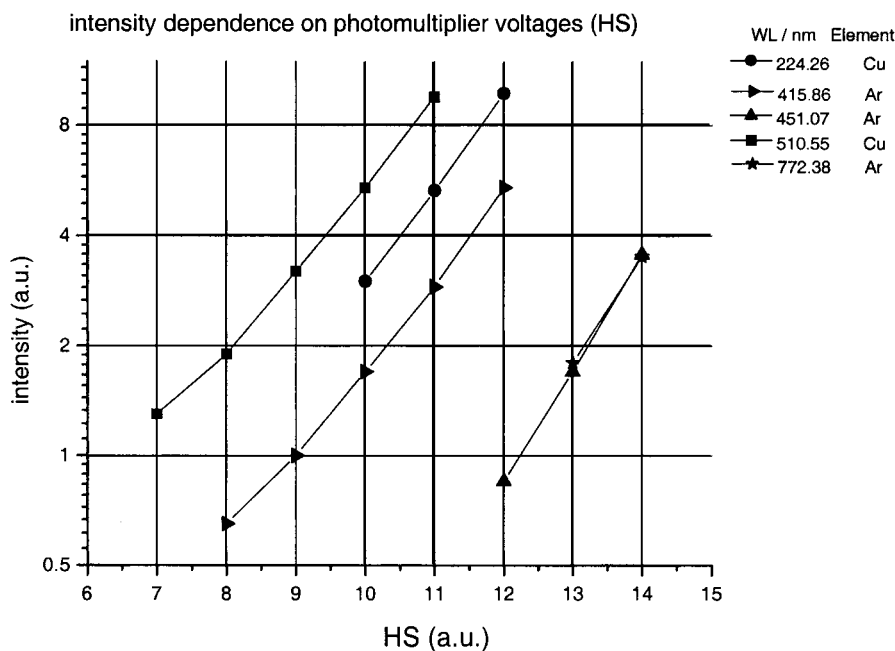


Fig. 1. Dependence of the line-intensity on the photomultiplier voltage (HS) for some lines.

Cu-samples had the same size ($20 \times 20 \times 1.25$ mm). Only a part of this sample, i.e. with diameter of 4 mm, was exposed to the discharge. One crater is sputtered in the center of each Cu-sample. To obtain the same plasma conditions, the distance between the anode and the Cu-sample must be the same for each measurement. For this purpose, we pressed the samples with constant pressure to the cathode plate. Deviations on the discharge conditions could be caused by samples with uneven surfaces. After each measurement, the GD source was cleaned with a special drilling tool. Nevertheless, small differences of the surface of the anode cannot be excluded. Additionally, the redeposition of sputtered material at the crater edge causes small differences in the gas flow and some temperature differences of sample, source and discharge gas also exist. All these factors lead to differences of the line intensities

between 5 and 10%, even if the same discharge conditions are applied.

The measurements are carried out in the following manner. First the monochromator is adjusted to one specific wavelength. Consequently, for each gas flow (200, 400 and 600 sccm), the voltages are set for sputtering (600, 800 and 1000 V). The measured current in flow and voltage constant mode is in the range between 5 and 50 mA. For one wavelength, all measurements are carried out when sputtering one specific sample and, therefore, the dependencies of line intensities at one wavelength on pressure and voltage are very reliable.

4. Results and discussion

4.1. Electrical characteristics

The measurements and calculations have been performed at three different pressures, and for each pressure at three different values of voltage and current. Fig. 2 shows the calculated (solid

Table 1
Calibration of pressure

Flow/sccm	200	400	600
Pressure/Pa	440	850	1184

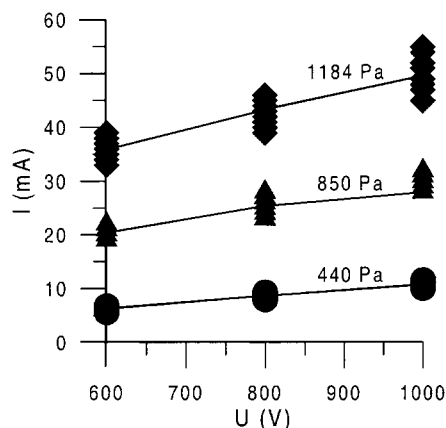


Fig. 2. Calculated (solid lines) and measured (symbols) electrical currents as a function of voltage at three different pressures. The calculations are performed at 600 V, 800 V and 1000 V, for each of the three indicated pressures, i.e. the same conditions as in the experiment.

lines) and measured (symbols) electrical current as a function of voltage at three different pressures. The electrical current in the model is calculated as the sum of the microscopic fluxes of the charged plasma particles (ions and electrons) and, since the current itself is a macroscopic quantity, it can be easily compared with experimental values. In order to obtain a calculated current value in agreement with the experimental data, we used the gas temperature as a fitting parameter. The values assumed for the gas temperature at the different conditions investigated are presented in Fig. 3. It appears that these gas temperature values are clearly above room temperature, and that they rise as a function of voltage and pressure (and, hence, also as a function of electrical current and power). This was also predicted in Bogaerts et al. [5] with a heat transfer equation, and it was also experimentally observed [6]. The model of Bogaerts et al. [5] calculates (by means of Monte Carlo models) the power input into the argon gas due to elastic (i.e. kinetic energy transfer) collisions of Ar^+ ions, fast Ar atoms, sputtered Cu atoms and electrons with the argon gas atoms. This power input is then used as the source term in the heat transfer equation. This model predicted that the gas temperature varies as a function of distance from the cathode, but we

assumed here for simplicity a constant value, and used it as a fitting parameter in the model instead of calculating it with the heat transfer equation. Indeed, we found that small variations in the gas temperature yielded quite large variations in the calculated current, due to a snowball-effect, i.e. a slightly lower gas temperature yields a slightly higher gas density and, hence, a slightly greater chance for collisions in the plasma; the extra ionization collisions give rise to more ions and electrons, which in turn create more ions and electrons (by secondary electron emission, and by ionization), and so on...; hence, this gives rise to more charged particles, and, therefore, a higher electrical current. Moreover, the results of the heat transfer model are subject to considerable uncertainties (due to uncertainties in the input data, such as the accommodation coefficients at the walls and the cathode temperature). Nevertheless, it appears that the gas temperature values assumed in the present study have realistic numbers, and show the same behavior as the predictions of the heat transfer model.

4.2. Erosion rates

Another macroscopic quantity which follows from the modeling calculations and which can

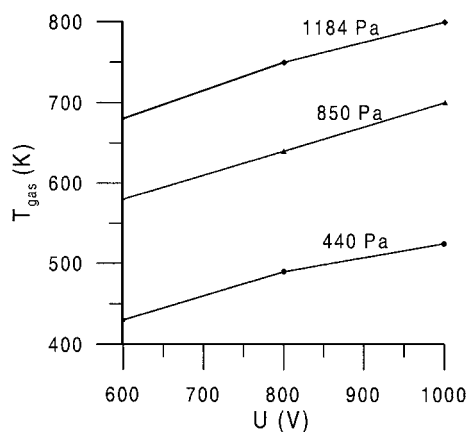


Fig. 3. Gas temperature values assumed in the model, in order to calculate electrical currents in correspondence with the experimental data. The calculations were performed at 600 V, 800 V and 1000 V, for each of the three indicated pressures.

easily be compared with experimental data is the erosion rate due to sputtering at the cathode. In the model it is calculated from the net sputtering flux (i.e. the flux of sputtered copper atoms minus the flux of redepositing copper atoms), as [7]:

$$ER = J_{\text{sput,net}} \frac{M}{N_A \rho}$$

where ER is the erosion rate (in cm/s), $J_{\text{sput,net}}$ is the net sputtering flux (in $\text{cm}^{-2} \text{s}^{-1}$), M and ρ are the atomic weight (in g/mol) and density of the sample material ($\rho_{\text{Cu}} = 8.92 \text{ g/cm}^3$ [8]), and N_A is Avogadro's number.

A large uncertainty in the model for the sputtered copper atoms, which directly affects the net sputtering flux and, hence, the calculated erosion rate, is the sticking coefficient of copper atoms at the walls, especially at the cathode. The sticking coefficient (a_0) determines the fraction of sputtered copper atoms bombarding a wall that are 'deposited' at the wall, i.e. $a_0 = 1$ means that 100% of the atoms are deposited, whereas $a_0 = 0$ indicates that all atoms are reflected. Data concerning the sticking coefficients for sputtered (i.e. mostly metallic) atoms at near thermal energies are very difficult to find in the literature. The data available are generally for gas molecules (H_2 , N_2 , rare gases) [9–11], but not for metallic atoms, which are normally not in the gas phase. Moreover, most data in the literature are for atoms with energies in the keV range [11], and not at thermal energies, which are of interest in our work. Finally, the analytical glow discharge operates under relatively high pressures (order of 1 torr and higher), whereas most previous studies specifically designed to observe this sticking phenomenon were carried out under 'clean' conditions and high vacuum. In Baker and Brink [12], the sticking coefficients of a potassium beam on several target materials in a vacuum chamber were measured. These values, together with some previously published data for several beam–target combinations, were used to derive some empirical relations among sticking coefficients, binding energies, and heats of formation. Sticking coefficient values, ranging between < 0.01 and 1.0 were tabulated for a range of beam–target combina-

tions (e.g. K, Rb, Cs, Ag, Ni, Zn, etc. atoms on brass, W, Al, Cu, Ag, glass, etc.) in vacuum [12].

In Bogaerts et al. [13], the effect of the sticking coefficient at cathode and anode walls on the sputtered atom density profiles was investigated, and it was found that this parameter has a considerable effect on the calculation results, especially at low sticking coefficient values [13]. Moreover, by comparison with experimental one-dimensional density profiles for sputtered lithium atoms, measured with concentration-modulated absorption spectrometry (COMAS), it appeared that sticking coefficients of lithium atoms in the range of 0.02–0.2 resulted in the best agreement with the experimental data [13]. Similarly, in van Veldhuizen and de Hoog [14], a comparison was made between calculated and experimental sputtered atom densities, and the authors found the best agreement when using sticking coefficients for copper atoms between 0.02 and 0.05. On the other hand, in a comparison between calculated two-dimensional density profiles of sputtered tantalum atoms with results obtained by laser-induced fluorescence (LIF) spectrometry [15], a sticking coefficient value of 0.5 at the cathode and anode appeared to give the best agreement.

This demonstrates that the sticking coefficients are subject to uncertainties and can vary, depending on the sputtered material, the surface structure and the temperature of the cell walls. Moreover, the surface structure can change during glow discharge operation [e.g., the walls can become dirty due to the deposition of sputtered material and/or the absorption of (impurity) gas atoms], possibly leading to sticking coefficients which are not constant over time, but can change during glow discharge operation. Therefore, we have investigated here the effect of the sticking coefficients on the calculated one-dimensional sputtered copper atom density profiles and on the calculated erosion rates, as is shown for one condition (i.e. intermediate pressure, voltage and current values: 850 Pa, 800 V and 25 mA) in Figs. 4 and 5, respectively. We assumed the same sticking coefficients for both cathode and anode walls. It appeared that the calculated density profile was especially affected by the sticking coefficient at the cathode and, to some extent, at the anode.

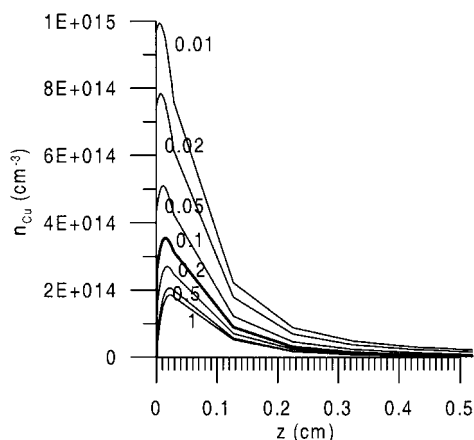


Fig. 4. One-dimensional density profiles of the sputtered copper atoms, calculated at different values of the sticking coefficient (only the first 5 mm from the cathode is shown), at 850 Pa, 800 V and 25 mA.

The calculated erosion rate, on the other hand, was only determined by the sticking coefficient at the cathode. It is clear that a lower sticking coefficient results in a higher calculated copper atom density and also in a higher erosion rate, because of less redeposition at the cathode. The effect is most pronounced at low values of the sticking coefficient. Moreover, Fig. 4 illustrates that very low sticking coefficient values result in a copper atom density profile with a maximum adjacent to the cathode, instead of a maximum at a

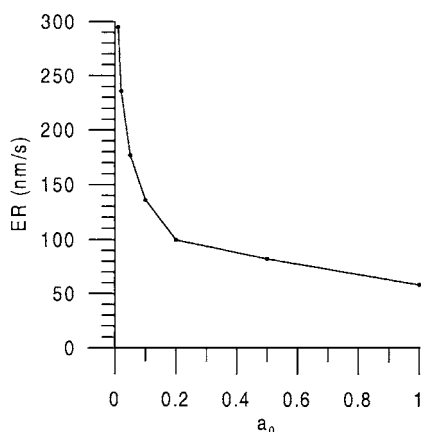


Fig. 5. Calculated erosion rates at different values of the sticking coefficient, at 850 Pa, 800 V and 25 mA.

few mm from the cathode, which is experimentally observed [15,16]. By comparison with the measured erosion rate at the condition under study (i.e. $ER_{\text{exp}} = 146 \text{ nm/s}$; see below), it appears that a value of 0.1 gives the best correspondence with the experimental data. Moreover, this value is realistic, in view of previous investigations [13,14], and it gives rise to a density profile with a maximum at a few mm from the cathode, in agreement with experimental observations [15,16]. Therefore, we have assumed this value of $a_0 = 0.1$ for all conditions investigated here.

The erosion rates calculated with our model in the way described above are plotted as a function of voltage at three different pressures in Fig. 6a (solid lines). The measured values at the same conditions are also presented in this figure (dashed lines + symbols). The agreement between calculated and measured erosion rates is reasonable. The absolute values are very similar, which is not too unexpected because the sticking coefficient was chosen in such a way that the calculated erosion rate corresponded to the experimental value, at least for one condition (i.e. intermediate pressure, voltage and current: 850 Pa, 800 V and 25 mA; see above). Looking at the effect of voltage and pressure, it appears that the pressure effect is correctly simulated, but the effect of the voltage is predicted somewhat too low, i.e. the calculated erosion rates do not rise as rapidly with voltage as the measured values. Indeed, the calculated erosion rates appear to rise in the same way as the electrical current (Fig. 2), whereas the experimental values behave more like the electrical power (i.e. the product of current and voltage) as a function of voltage (see Fig. 7 below). It is indeed expected that the erosion rates increase with the product of voltage and current, i.e. a higher current results in higher fluxes of bombarding species at the cathode, and a higher voltage results in higher energies of the bombarding species, which both give rise to more sputtering (at least in the energy range corresponding to typical voltages in analytical glow discharges). The reason for the discrepancy in the calculated and experimental results is not completely clear, but it might be attributed to the assumed gas temperature values. Indeed, based on earlier predictions

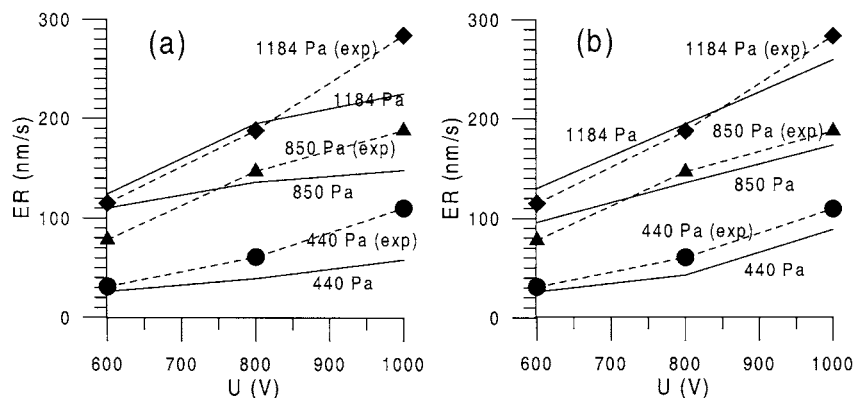


Fig. 6. Calculated (solid lines) and measured (symbols + dashed lines) erosion rates as a function of voltage at three different pressures. Fig. 6a presents the calculated results assuming a rising gas temperature as a function of voltage (see Fig. 3), whereas in Fig. 6b, the calculation results are illustrated assuming a constant gas temperature.

with the heat transfer equation [5] and on experimental observations [6], we assumed that the gas temperature increases slightly as a function of voltage (see Fig. 3), in order to calculate electrical currents in agreement with the experimental data. However, a higher gas temperature yields a lower gas density at a constant pressure value, according to the ideal gas law ($n = N/V = p/kT$), resulting in less collisions in the plasma and, hence, less formation of argon ions and fast argon atoms bombarding the cathode for sputtering and, therefore, a lower erosion rate. To check the above idea, we have repeated our calculations assuming a constant gas temperature as a function of voltage, i.e. only varying as a function of pressure (430 K at 440 Pa, 640 K at 850 Pa and 750 K at 1184 Pa), and the resulting erosion rates are presented in Fig. 6b. It is clear that the calculated erosion rates are now in much better agreement with the experimental values, both for the absolute values and for the effect of voltage and pressure. This suggests that the gas temperature would be independent of the voltage. However, the latter assumption would yield a too rapid increase of the electrical current as a function of voltage, as was indeed (incorrectly) predicted by Bogaerts and Gijbels [2]. It appears indeed that in a Grimm-type source, the measured current–voltage curves always exhibit a convex shape [17]. Moreover, from theoretical

predictions [5] and experimental observations [6], it is expected that the gas temperature does increase as a function of voltage. Summarizing, it appears that our calculations cannot yet simultaneously predict the correct behavior of both the electrical current and the erosion rate as a function of voltage. This means that there is still some voltage effect not correctly described in the model. Probably, the gas temperature does increase slightly as a function of voltage, but maybe not so pronounced as was illustrated in Fig. 3. Moreover, the fact that the gas temperature was assumed to

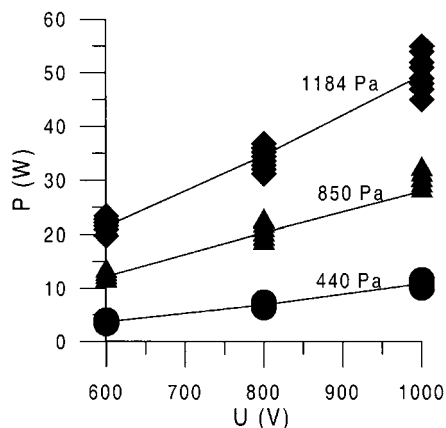


Fig. 7. Calculated (solid lines) and measured (symbols) values of the electrical power as a function of voltage at three different pressures.

be constant throughout the whole discharge region, in contrast to theoretical predictions [5] and experimental observations [6], might be responsible for the incorrect description of the voltage effect. Some authors [18] use the effective ion induced secondary electron emission coefficient as a fitting parameter, in order to calculate the correct currents at a certain voltage, because this parameter is subject to considerable uncertainties. If this approach would have been applied here, thereby assuming a constant gas temperature, both the voltage-behavior of the electrical current and of the erosion rate could have been correctly predicted, but in order to reach this, the assumed ion-induced secondary electron emission coefficient would have to drop slightly as a function of voltage, and this is contrary to our expectations (i.e. it would be expected that a higher voltage yields higher ion energies and, therefore, slightly more secondary electron emission [19]). On the other hand, the secondary electron emission coefficient will also be a function of the cathode temperature, but the exact dependence is not known. We assumed a constant value for the secondary electron emission coefficient at all conditions, which is clearly an approximation. This might be responsible for the small deviation in the calculated and measured results. In the future, it might make sense to use the secondary electron emission coefficient as a fitting parameter. In any case, more detailed investigations on the exact values of the secondary electron emission coefficients will be needed [20]. Moreover, accurate measurements of the gas temperature in the plasma would also be of valuable help to verify the model calculations.

In any case, we hope that from the small discrepancy between the modeling calculations and experimental observations, we will be able to find the missing points in our calculations, to improve the model, and to make more realistic predictions in the future. Nevertheless, it should be mentioned that, even when the gas temperature is assumed to be a function of voltage, like that illustrated in Fig. 3, the agreement between calculated and measured erosion rates (Fig. 6a) is not that bad.

4.3. Optical emission intensities

The model is also able to calculate the optical emission intensities of argon and copper lines [21]. The latter are calculated from the level populations of the excited argon and copper levels, multiplied with the Einstein transition probabilities for radiative decay. In our model, 64 argon atom excited levels, eight copper atom and seven Cu^+ ion excited levels are taken into account, and from them, the optical emission intensities of 605 ArI lines and 103 CuI and CuII lines can be calculated. This large number of levels and optical emission lines illustrates the complexity and comprehensiveness of the model. The optical emission intensities of ArII lines cannot yet be calculated with the present model, since the argon collisional–radiative model considers only argon atomic levels. For the purpose of the present comparison, we have selected some ArI, CuI and CuII lines originating from different excited levels, in order to check whether the calculations correctly describe the various populating and depopulating mechanisms for different levels. The following three figures illustrate some ArI, CuII and CuII line intensities as a function of voltage at three different pressures. The calculated intensities are represented with the solid lines (left axis), whereas the experimental data are presented with symbols and dashed lines (right axis). In analogy to the erosion rates, we have calculated the optical emission intensities with and without varying the gas temperatures as a function of voltage, and the results are represented with the thin and thick solid lines, respectively. It is clear that the calculation results with a constant gas temperature (thick solid lines) are in much better agreement with the experimental data. Therefore, in the following, we will only discuss these results. The thin solid lines are only included in the figure to show that the agreement is less satisfactory, and to illustrate that it is not at all straightforward to reach good agreement between model and experiment (because even small variations in the model input data can lead to large discrepancies with the experimental results).

Fig. 8 illustrates the intensities of two ArI lines,

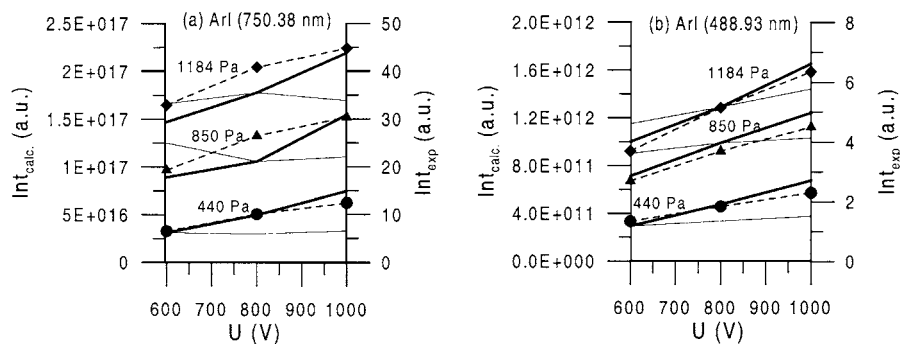


Fig. 8. Calculated (solid lines, left axis) and measured (symbols + dashed lines, right axis) optical emission intensities of two ArI lines, as a function of voltage at three different pressures. The thick and thin solid lines represent the calculation results with and without keeping the gas temperature constant as a function of voltage.

i.e. the ArI 750.38 nm line, which corresponds to a 4p–4s transition (Fig. 8a) and the ArI 488.93 nm line, which corresponds to a 7d–4p transition (Fig. 8b). It is indeed apparent that the results calculated, assuming a constant gas temperature, yield a much better agreement with experimental data. The two lines presented in Fig. 8a,b originate from a low and a high argon excited level, respectively, but they show a similar behavior as a function of voltage and pressure. We found indeed that all ArI lines rise more or less to the same extent as a function of voltage and pressure.

In Fig. 9, the intensities of three CuI lines are presented, i.e. the CuI 261.84-nm line (corresponding to a 5p–4s² transition; Fig. 9a), the CuI 324.75-nm line (a resonance line, originating from a 4p level and decaying to the copper ground state (= 4s level); Fig. 9b), and the CuI 578.21-nm line (corresponding to the transition 4p–4s²; Fig. 9c). Again, the agreement with experiment appears to be better for the calculations where the gas temperature was assumed to be constant (except at a pressure of 440 Pa). The agreement between model and experiment is reasonable for the two non-resonant lines (Fig. 9a,c), but it is not yet satisfactory for the 324.75-nm resonant line, at least for the effect of pressure, which is too small in the calculation results compared to the experimental data. The reason for the small effect of pressure in the calculation results is because this line is subject to self-absorption. This

means that a considerable fraction of the emitted radiation from the upper level is reabsorbed by the lower level, so that the final intensity of this line is significantly reduced. This phenomenon of self-absorption occurs only for transitions to the ground state, i.e. so-called resonant lines, because the level population of the ground state is large enough to reabsorb radiation. It is to be expected that this effect of self-absorption is larger at high pressures, where the copper atomic ground state has a high density. This explains why the net intensity of the 324.7-nm resonance line rises only slightly with pressure. However, it appears that the effect of self-absorption is overestimated in the model. This phenomenon is, indeed, quite complicated to describe, and the formulas used [22] are only approximate. Hence, it is quite possible that this effect is not yet correctly described, and that the intensities of the resonant lines, therefore, cannot be correctly predicted. On the other hand, the effect of voltage on the resonant line intensities seems to be correctly described. Moreover, the intensities of all other CuI lines (not only the ones shown in Fig. 9a,c, but also all other non-resonant CuI lines) were found to be correctly calculated in the model. From the comparison of Fig. 9 with Fig. 8, it is clear that the CuI lines (except the resonant lines) rise more rapidly with voltage than the ArI lines, i.e. the ArI lines rise to the same extent with voltage as the electrical current (cf. Fig. 2), whereas the CuI

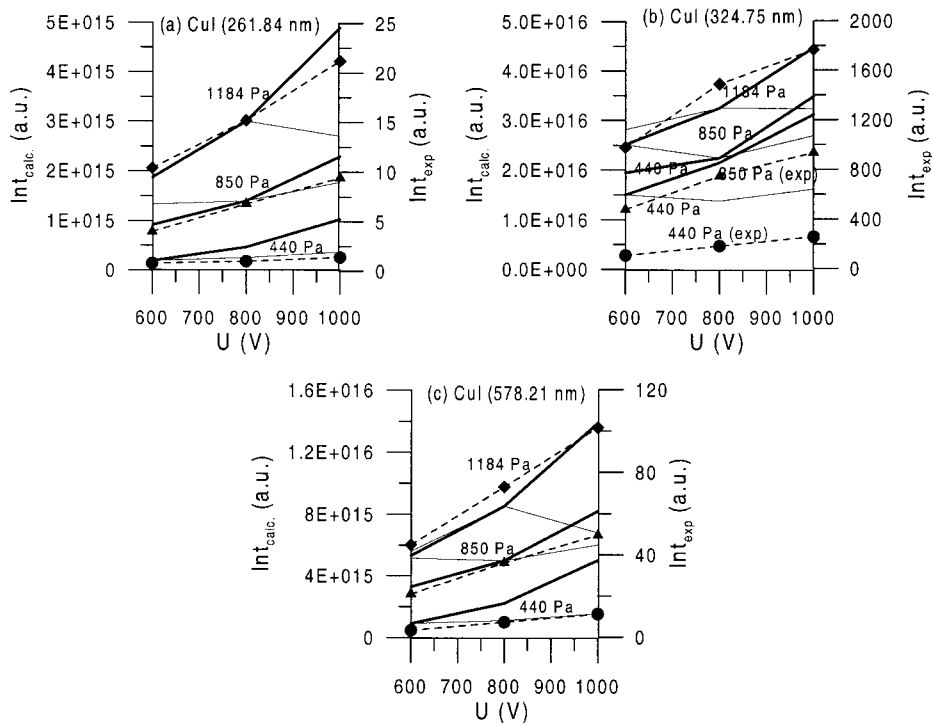


Fig. 9. Calculated (solid lines, left axis) and measured (symbols + dashed lines, right axis) optical emission intensities of three CuI lines, as a function of voltage at three different pressures. The thick and thin solid lines represent the calculation results with and without keeping the gas temperature constant as a function of voltage.

lines show a similar behavior as the electrical power vs. voltage (cf. Fig. 7). Indeed, the ArI line intensities are the result of the argon ground state density [i.e. constant as a function of voltage when the gas temperature is assumed to be constant (thick solid lines)] multiplied with the excitation rate (which increases with the voltage). On the other hand, the CuI line intensities result from the product of the copper ground state density and the excitation rate, which both increase with voltage. Therefore, it is indeed expected that the CuI line intensities rise more rapidly with voltage than the ArI line intensities.

Finally, Fig. 10 shows the intensities of two CuII lines, i.e. the CuII 221.81-nm line (corresponding to a $4p-4s$ transition; Fig. 10a) and the CuII 224.7-nm line (Fig. 10b). The latter line also corresponds to a $4p-4s$ transition, but the upper $4p$ level (i.e. the $4p^3P_2$ level) is selectively populated by asymmetric charge transfer with argon

ions. The effect of voltage and pressure on these two CuII line intensities seems to be more or less correctly predicted by the model when the gas temperature was assumed constant as a function of voltage. The same result was found for all other CuII lines.

Hence, it appears that the model satisfactorily predicts the effect of voltage and pressure on the optical emission intensities of ArI, CuI and CuII lines, especially when the gas temperature was assumed constant. This demonstrates that the many populating and depopulating processes of these levels are correctly described in the model. The absolute values of the optical emission intensities cannot yet be compared with the experimental data, because the latter are also subject to wavelength-dependent effects (such as the sensitivity of the monochromator). However, the qualitative trends (i.e. high calculated intensities correspond to high measured intensities, and vice versa)

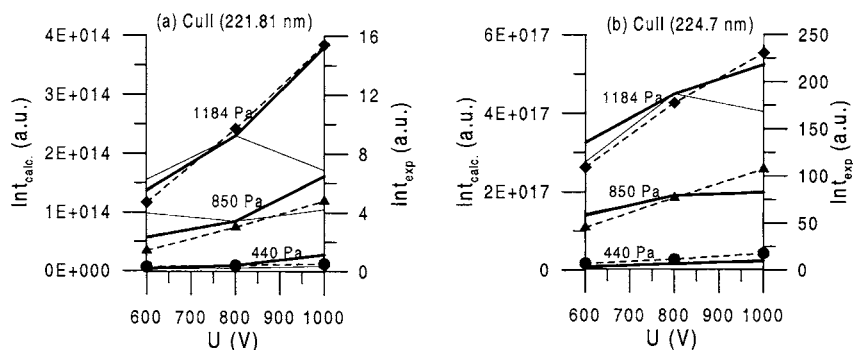


Fig. 10. Calculated (solid lines, left axis) and measured (symbols + dashed lines, right axis) optical emission intensities of two CuI lines, as a function of voltage at three different pressures. The thick and thin solid lines represent the calculation results with and without keeping the gas temperature constant as a function of voltage.

are also in reasonable agreement. Finally, it should be mentioned that the calculated intensities of various ArI, ArII and CuI lines as a function of distance from the cathode were also found to be in excellent agreement with experimental data, and at various voltage–pressure–current conditions [23], which also demonstrates that the populating and depopulating processes are correctly taken into account.

5. Conclusion

In this paper, a comparison is made between modeling calculations and experimental data for the electrical characteristics (current as a function of voltage and pressure), the erosion rates and the optical emission intensities of various ArI, CuI and CuII lines, at a range of voltages and pressures in a direct current glow discharge, in order to verify the model calculations and to show the features and limitations of the model. Because of many uncertainties in the model input data which can largely affect the calculation results (e.g. the gas temperature, but also some cross sections, the ion-induced secondary electron emission coefficient, etc.), an exact quantitative agreement can only be reached if one of these input parameters is allowed to be adjusted. In this work, we adjusted the gas temperature, in order to calculate the electrical current in agreement with the experimental values. The gas tempera-

ture was found to be clearly above room temperature, ranging from 430 K (at 440 Pa, 600 V and 6 mA) to 800 K (at 1184 Pa, 1000 V and 50 mA). These absolute values and the increasing behavior as a function of voltage, pressure and current are realistic in view of earlier theoretical predictions [5] and experimental observations [6]. However, with these gas temperatures, the calculated erosion rates and optical emission intensities did not increase as rapidly with voltage as the experimental data. Indeed, the higher gas temperatures at high voltage yield lower gas densities at constant pressure (according to the ideal gas law), resulting in less collisions, less sputtering (hence, lower erosion rates) and less excitation (hence, lower optical emission intensities). When repeating the calculations with a constant gas temperature as a function of voltage, the voltage-effect on the calculated erosion rates and optical emission intensities was found to be in much better agreement with the experimental data. This suggests that (i) either the gas temperature should be constant as a function of voltage [however, this is in contrast to theoretical predictions and experimental observations, and moreover, the current would then increase too rapidly with voltage, see [2]; so another effect would then be responsible for the experimentally observed small slope (and even saturation) in the current–voltage characteristics] or (ii) the gas temperature rises slightly with voltage, but then another effect must compensate for the low sputtering and excitation rates.

In any case, it is clear that the numerical model cannot yet completely correctly predict the voltage effect simultaneously on both the electrical current, and the erosion rate and optical emission intensities, and that a certain aspect is not yet sufficiently accurately described in the model. Based on the present comparison, in combination with some more detailed investigations (e.g. measurements of the gas temperature as a function of voltage might be helpful), we hope to discover this limitation in the model. On the other hand, it should be mentioned that the overall agreement between calculated and measured results is already quite satisfactory, certainly in view of the many uncertainties in the input data and the complexity of the model calculations. In general, it can, therefore, be concluded that the model presents a realistic picture of a direct current glow discharge. In the near future, a similar comparison between modeling and experimental results will be performed for a radio-frequency glow discharge.

Acknowledgements

A. Bogaerts is indebted to the Flemish Fund for Scientific Research (FWO-Flanders) for financial support. The authors also acknowledge financial support from the Federal Services for Scientific, Technical and Cultural Affairs (DWTC/SSTC) of the Prime Minister's Office through IUAP-IV (Conv. P4/10). This cooperation was carried out in the framework of an EC Thematic Network on Glow Discharge Spectroscopy for Spectrochemical Analysis (SMT4-CT98-7517). Finally, A. Bogaerts would like to thank Z. Donko for the interesting discussions.

References

- [1] A. Bogaerts, R. Gijbels, Modeling of argon direct current glow discharges and comparison with experiments: how good is the agreement? *J. Anal. At. Spectrom.* 13 (1998) 945–953.
- [2] A. Bogaerts, R. Gijbels, Comprehensive description of a Grimm-type glow discharge source used for optical emission spectrometry: a mathematical simulation, *Spectrochim. Acta Part B* 53 (1998) 437–462.
- [3] W. Grimm, Patent 1 589 389, 1967.
- [4] V. Hoffmann, H.-J. Uhlemann, F. Präßler, K. Wetzig, D. Birus, New hardware for radiofrequency powered glow discharge spectroscopies and its capabilities for analytical applications, *Fresenius J. Anal. Chem.* 355 (1996) 826–830.
- [5] A. Bogaerts, R. Gijbels, V.V. Serikov, Calculation of gas heating in direct current argon glow discharges, *J. Appl. Phys.* 87 (2000) 8334–8344.
- [6] N.P. Ferreira, H.G.C. Human, L.R.P. Butler, Kinetic temperatures and electron densities in the plasma of a side view Grimm-type glow discharge, *Spectrochim. Acta Part B* 35 (1980) 287–295.
- [7] A. Bogaerts, R. Gijbels, Calculation of crater profiles on a flat cathode in a direct current glow discharge, and comparison with experiment, *Spectrochim. Acta Part B* 52 (1997) 765–778.
- [8] R.C. Weast, M.J. Astle, *CRC handbook of Chemistry and Physics*, 63rd Edition, CRC Press, Boca Raton, 1982–1983.
- [9] R.T. Brackmann, W.L. Fite, Condensation of atomic and molecular hydrogen at low temperatures, *J. Chem. Phys.* 34 (1961) 1572–1579.
- [10] J.N. Smith, W.L. Fite, Reflection and dissociation of H₂ on tungsten, *J. Chem. Phys.* 37 (1962) 898–904.
- [11] W. Eckstein, H. Verbeek, Reflection of H, D, and He from C, Ti, Ni, Mo, W, and Au, *J. Nucl. Mater.* 76 & 77 (1978) 365–369.
- [12] F.S. Baker, G.O. Brink, Adsorption of potassium beams on surfaces, *J. Chem. Phys.* 37 (1962) 1012–1017.
- [13] A. Bogaerts, J. Naylor, M. Hatcher, W.J. Jones, R. Mason, Influence of sticking coefficients on the behavior of sputtered atoms in an argon glow discharge: modeling and comparison with experiment, *J. Vac. Sci. Technol. A* 16 (1998) 2400–2410.
- [14] E.M. van Veldhuizen, F.J. de Hoog, Analysis of a Cu–Ne hollow cathode glow discharge at intermediate currents, *J. Phys. D: Appl. Phys.* 17 (1984) 953–968.
- [15] A. Bogaerts, E. Wagner, B.W. Smith, J.D. Winefordner, D. Pollmann, W.W. Harrison, R. Gijbels, Three-dimensional density profiles of sputtered atoms and ions in a direct current glow discharge: experimental study and comparison with calculations *Spectrochim. Acta Part B* 52 (1997) 205–218.
- [16] N.P. Ferreira, H.G.C. Human, A study of the density of sputtered atoms in the plasma of the modified Grimm-type glow discharge source *Spectrochim. Acta Part B* 36 (1981) 215–229.
- [17] V. Hoffmann, F. Praessler, K. Wetzig, '30 Jahre Grimmsche Glimmentladungsquelle: Untersuchungen der Entladungsparameter, *Proceedings CANAS 1997*, ISSN 0945-3254 (1998) 29–39.
- [18] K. Kutasi, Z. Donko, Hybrid model of a plane-parallel hollow-cathode discharge, *J. Phys. D: Appl. Phys.* 33 (2000) 1081–1089.
- [19] A.V. Phelps, Z.Lj. Petrovic, Cold-cathode discharges and breakdown in argon: surface and gas phase produc-

- tion of secondary electrons, *Plasma Sources Sci. Technol.* 8 (1999) R21–R44.
- [20] Z. Donko, On the apparent secondary electron emission coefficient in argon glow discharges. Proceedings of the XXV ICPIG Conference, Nagoya, Japan (2001).
- [21] A. Bogaerts, R. Gijbels, Argon and copper optical emission spectra in a Grimm glow discharge source: mathematical simulations and comparison with experiment, *J. Anal. At. Spectrom.* 13 (1998) 721–726.
- [22] A. Bogaerts, R. Gijbels, R.J. Carman, Collisional–radiative model for the sputtered copper atoms and ions in a direct current argon glow discharge, *Spectrochim. Acta Part B* 53 (1998) 1679–1703.
- [23] A. Bogaerts, Z. Donko, K. Kutasi, G. Bano, N. Pinhao, M. Pinheiro, Comparison of calculated and measured optical emission intensities in a direct current argon–copper glow discharge, *Spectrochim. Acta Part B* 55 (2000) 1465–1479.